

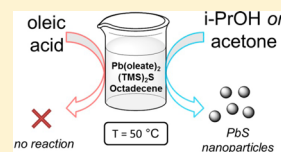
Formation of Ultrasmall PbS Nanocrystals in Octadecene at Mild Temperature Promoted by Alcohol or Acetone Injection

Artsiom Antanovich, Anatol Prudnikau, and Mikhail Artemyev*

Institute for Physico-Chemical Problems, Belarusian State University, Leningradskaya str. 14, Minsk 220030, Belarus

Supporting Information

ABSTRACT: The formation of ultrasmall PbS nanoparticles by the reaction of lead oleate with bis(trimethylsilyl) sulfide in octadecene at a temperature as low as 50 °C can be strongly promoted by addition of protic solvents (alcohols, water) or acetone. The proposed mechanism involves formation of the $\text{Pb(oleate)}_2\text{-(TMS)}_2\text{S}$ complex which upon the injection of a proper solvent forms highly reactive Pb- and S-containing intermediates. The different reactive ability of these intermediates depending on the type of promoter allows one to prepare PbS QDs with different size. Such a mild-temperature process is useful for production of ultrasmall monodisperse PbS colloidal quantum dots due to suppressed recrystallization of PbS nanoparticles.



INTRODUCTION

Lead sulfide and lead selenide colloidal nanocrystals are popular objects to study the basic optical properties of semiconductor quantum dots (QDs) and utilize them in photovoltaic structures due to the ability for multiexciton generation and large exciton Bohr radii.^{1–4}

PbS nanoparticles were prepared by numerous approaches, including chemical growth inside polymeric^{5,6} or glass hosts,⁷ hydrothermal single precursor route,⁸ colloidal synthesis in aqueous media,^{9,10} and organic solvents.^{11–14} Earlier, Joo et al.¹⁴ demonstrated nonaqueous synthesis of PbS nanocrystals by the reaction between oleylamine solution of PbCl_2 and elemental sulfur at 220 °C. Using this procedure, they managed to obtain PbS particles ranging from 6 to 13 nm. Later, Cademartiri et al.¹¹ modified this protocol by decreasing the reaction temperature to 100 °C, which gave 4.2–6.4 nm sized PbS QDs emitting between 1245 and 1625 nm with photoluminescence (PL) quantum yield up to 40%. Moreels et al.¹⁵ showed that the addition of TOP to the reaction mixture allowed to extend the range of available sizes to 3–10 nm, but more importantly, they showed that oleylamine ligands exhibit fast exchange between solution and the surface of PbS nanoparticles. In contrast, molecules of oleic acid are tightly bound to the surface, thus providing better surface passivation which produces considerably higher PL quantum yield.

One of the extensively used method for the synthesis of PbS quantum dots involves injection of bis(trimethylsilyl) sulfide ($(\text{TMS})_2\text{S}$) as a sulfur precursor into the solution containing lead oleate at elevated temperatures (typically 80–140 °C).^{12,16–19} This procedure yields PbS QDs ranging from 2.6 to 7.2 nm in size with clearly pronounced excitonic absorption peaks between 800 and 1800 nm, relatively narrow size distribution, and ~20% PL quantum yield. An extensive study on the PbS QDs synthesis by the reaction between lead salts and $(\text{TMS})_2\text{S}$ was conducted by Liu et al.¹⁶ They studied the influence of the oleic acid:Pb:S ratio, various capping ligands and temperature on the kinetic parameters of reaction. They

demonstrated that high Pb-to-S ratio inhibits the PbS nanoparticles growth even at elevated temperatures as high as 70 °C.

As one can see, synthetic protocols concerning the preparation of quantum dots ranging from 2 to 10 nm are well documented. Although ultrasmall PbS and PbSe QDs with diameters less than 2 nm are of great interest since they open the possibility to study nanoparticles in extreme quantum confinement regime, information on their synthesis, however, is still scarce

Here, we demonstrate that the reaction between lead oleate and $(\text{TMS})_2\text{S}$ can be carried out even at a mild temperature of 50 °C, promoted by addition of hydroxyl-containing solvents, like isopropyl alcohol. We proposed the mechanism based on the formation of intermediate complex between $(\text{TMS})_2\text{S}$ and lead salt followed by hydroxyl attack on the Si–S bond.

MATERIALS AND METHODS

Materials. Lead oxide ($\geq 99.0\%$, Sigma-Aldrich), cadmium oxide ($\geq 99.0\%$, Fluka), octadecene-1 (ODE, 90%, Sigma-Aldrich), bis(trimethylsilyl) sulfide ($(\text{TMS})_2\text{S}$, Sigma-Aldrich, synthesis grade), oleic acid (OA, 90%, Sigma-Aldrich), heptane, and hexane were used as received. Isopropyl alcohol, acetone, and tetrahydrofuran (THF) were distilled, dried, and stored over A4 molecular sieves prior to use.

Characterization Technique. Optical absorption spectra were recorded using a HR-2000+ spectrometer (Ocean Optics) with Ocean Optics DH-2000 white light source. PL and PLE measurements were conducted with a Jobin-Yvon Fluoromax-2 spectrofluorometer. Energy dispersive X-ray spectroscopy analysis was performed using a scanning electron microscope LEO-1420, equipped with an energy dispersion spectrometer. Room temperature X-ray diffraction analysis of powdered

Received: March 21, 2014

Revised: August 22, 2014

Published: August 26, 2014



samples of PbS QDs was carried out with Empyrean Series 2 diffractometer (Cu $K\alpha_1$ line).

Synthesis of PbS Nanoparticles. We adopted the protocol described by Hines and Scholes¹² with some modifications. In brief, a 100 mL three-necked flask was loaded with 50 mL of ODE, 112 mg (0.5 mmol) of PbO, and 675 μ L (2.1 mmol) of oleic acid. Then the reaction mixture was purged with argon and heated to 50 °C. At this point 220 μ L of 0.47 M solution of (TMS)₂S in hexane was swiftly introduced into the as-formed Pb(oleate)₂ solution, thus yielding the resultant molar ratio between components OA:Pb:S = 22:5:1. It worth noting that after the (TMS)₂S reaction the mixture remained colorless. In order to induce nanoparticles' formation, 3 mL of isopropanol was added into the flask. Soon after the alcohol injection the color of the reaction solution changed to yellowish and after 5 min dark brown. The flask was heated for another 10 min to increase the reaction yield. When the reaction was stopped, as-formed nanocrystals were isolated by the addition of an excessive amount of isopropanol–acetone mixture followed by prolonged centrifugation at 5000 rpm. A deposit of PbS QDs was additionally washed several times with isopropanol and dried to powder for subsequent XRD and elemental analysis.

RESULTS AND DISCUSSION

The crystalline nature and elemental composition of the prepared nanoparticles were examined by XRD and EDX-measurements. The X-ray diffractogram of the nanoparticles along with JCPDS data for lead sulfide are shown in Figure 1.

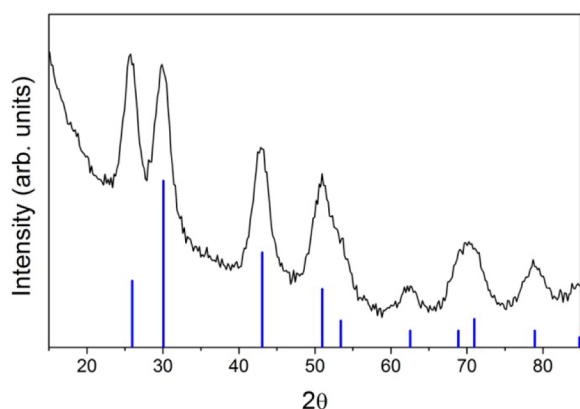


Figure 1. XRD pattern of the prepared PbS powder (black line) with standard data (JCPDS pdf #050592; blue bars) provided for a reference.

As one can see, the presented XRD pattern correlates well with provided reference data, thus confirming that as-prepared nanoparticles consist of lead sulfide with rock-salt structure. EDX measurements (see Figure S1 in the Supporting Information) also confirm that obtained QDs consist of lead and sulfur. The presence of small silicon amounts detected by EDX could be assigned to the trimethylsilyl moieties left after (TMS)₂S decomposition. A representative TEM image of PbS nanoparticles prepared by this method is presented in Figure S2 of the Supporting Information.

Figure 2 shows optical absorption, PL, and PLE spectra of the as-obtained PbS nanoparticles dispersed in chloroform. On the absorption spectrum one can see broad excitonic peak at 650 nm. Using this value and the equation from ref 21, the

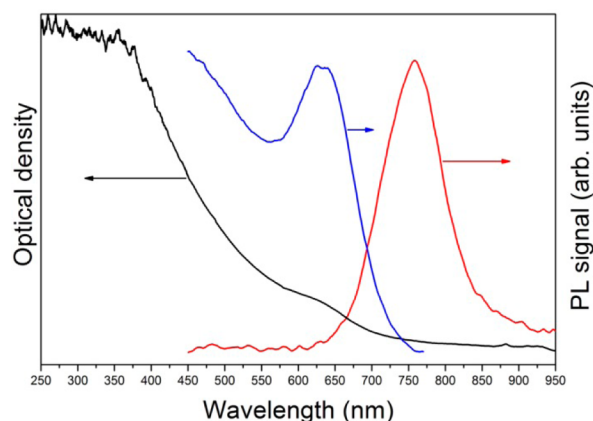


Figure 2. Optical absorption (black curve), photoluminescence ($\lambda_{\text{exc}} = 400$ nm; red curve) and photoluminescence excitation ($\lambda_{\text{em}} = 760$ nm; blue curve) spectra of PbS nanoparticles dissolved in chloroform.

diameter of the prepared PbS nanoparticles can be estimated to be ca. 1.5 nm, which is close enough to the value of 1.7 nm obtained from TEM measurements of the PbS nanoparticles with similar absorption spectrum synthesized in a polymer host.⁶

The solution of the as-obtained PbS under UV-illumination ($\lambda_{\text{exc}} = 400$ nm) showed no luminescence (not shown), which could be explained by poor passivation of sulfur surface atoms that results in PL quenching.¹⁸ Indeed, after the addition of TOP to the solution of nanoparticles, appearance of the bright luminescence band centered at 760 nm is observed. One can notice that the Stokes shift is relatively large (about 110 nm or ca. 280 meV), which was shown to be a characteristic feature for small PbS nanocrystals due to the appearance of size-dependent electron state within the band gap.¹⁹ The PLE spectrum follows the absorption one, thus indicating that luminescence is attributed to the PbS nanoparticles.

In order to study the protocol under consideration in more details, we conducted a series of experiments in a 1 cm optical quartz cuvette in air. A quartz cuvette was placed into thermostated cuvette holder (Ocean Optics CUV-ALL-UV) connected by optical fibers to the white light source and spectrometer. It worth mentioning that as the synthesis carried out under argon proceeds in a similar fashion, the influence of the air moisture and oxygen in our experiments can be neglected. A stock solution of lead oleate was prepared by reacting 11 mg (0.05 mmol) of PbO in 10 mL of octadecene containing 67.5 μ L (0.21 mmol) of oleic acid. Then, 1.5 mL of obtained Pb(oleate)₂ solution was transferred into 1 cm quartz cuvette and heated to 50 °C. The temperature of reaction mixture was controlled with a glass-covered thermocouple. When the temperature became stable, the thermocouple was removed and 30 μ L of 0.047 M solution of (TMS)₂S in hexane was injected into the Pb(oleate)₂ solution with stirring. Ten seconds after, 1 mL of different reaction promoter, isopropyl alcohol, acetone, or THF, was injected to the reaction mixture with stirring. The optical absorption spectra of the reaction mixture were recorded before and after (TMS)₂S addition and a certain period after addition of a promoter. The kinetics of reaction was analyzed from time-growing optical absorption of formed PbS QDs. It should be noted that reactant concentrations were changed (however, components molar ratio was set the same) in order to obtain less optically dense

solution and hence to provide the ability to study reaction using optical absorption spectroscopy.

Figure 3 shows optical absorption spectra at $T = 50\text{ }^{\circ}\text{C}$ of $\text{Pb}(\text{oleate})_2$ solution in ODE before (blue curve) and after

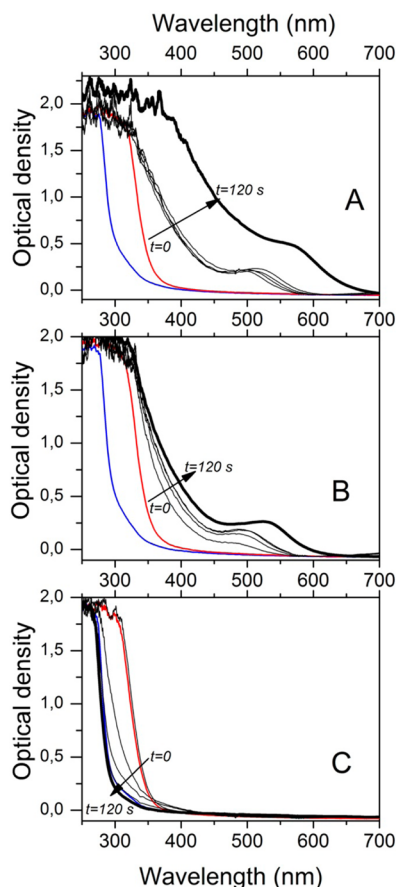


Figure 3. Optical absorption spectra of $\text{Pb}(\text{oleate})_2$ solution in ODE (blue line), after $(\text{TMS})_2\text{S}$ addition (red line), and after subsequent promoter injection: 1–5 s (thin black lines), 120 s (bold black line). Panel A: isopropyl alcohol; panel B: acetone; panel C: THF as a reaction promoters. The temperature of reaction $T = 50\text{ }^{\circ}\text{C}$.

$(\text{TMS})_2\text{S}$ addition (red curve) followed by different promoter injection (black curves).

It should be outlined that no PbS formation was detected even at $T = 60\text{ }^{\circ}\text{C}$ for at least 20 min after the addition of $(\text{TMS})_2\text{S}$. This result may seem to be in contradiction with earlier reports on the synthesis of PbS QDs at mild temperature.^{16,17} We attribute this discrepancy to much higher OA-to-Pb ratio in our case. The increase in Pb:S and OA:Pb ratios was shown to slow down the growth of PbS nanoparticles.^{16,18} Injection of $(\text{TMS})_2\text{S}$ into the reaction mixture results in the induced optical absorption below $\lambda \approx 350\text{ nm}$, which can be attributed to the formation of complex between $(\text{TMS})_2\text{S}$ and lead oleate (red curves in Figure 3). The addition of isopropyl alcohol to the reaction mixture initiates rapid formation and growth of PbS QDs which is seen as absorption continuum below 400 nm with characteristic first excitonic band continuously shifted from 500 to 580 nm (Figure 3a), which corresponds to PbS nanoparticles of ca. 1.2–1.3 nm in diameter.²¹ A similar effect was observed for other alcohols like 1-octanol and 1-butanol with small variations in the reaction speed. Addition of acetone instead

of alcohol also promotes the reaction, but the formation and growth of PbS QDs is going much slowly (Figure 3b). Figure 3c also demonstrates that the addition of polar aprotic solvent THF does not initiate the reaction within 2 min at $T = 50\text{ }^{\circ}\text{C}$. It is interesting to note that the addition of THF results in depletion of induced optical absorption below $\lambda \approx 350\text{ nm}$. The mechanism for this effect will be discussed below.

In order to examine the kinetics of PbS formation in the presence of different solvents, we plotted the optical absorption of solution at $\lambda = 420\text{ nm}$ versus the reaction time for four different solvents: dry isopropyl alcohol, dry acetone, dry THF, and as-received THF (Figure 4). The selected spectral region is

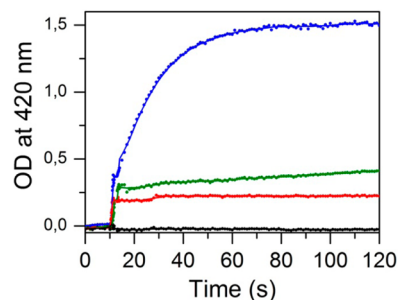


Figure 4. Evolution of optical density at $\lambda = 420\text{ nm}$ of the reaction mixture after different promoter injection: dry isopropyl alcohol (blue line), dry acetone (green line), dry THF (black line), and as-received THF (red line). The promoter injection was done at $t = 10\text{ s}$. The temperature of reaction $T = 50\text{ }^{\circ}\text{C}$.

close to the energies of continuum of states in PbS QDs. Since the optical density of QDs ensemble in diluted systems measured far above the band gap of the bulk material, i.e. in the continuum of states, is proportional to the total number of atoms in the ensemble and does not depend on the size or shape,²² the value of OD at $\lambda \approx 420\text{ nm}$ can be used for rough estimation of the chemical reaction yield.

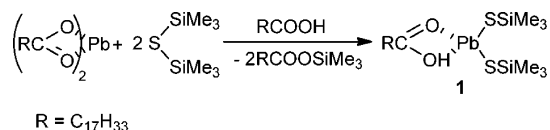
From Figure 4 we may see that the injection of isopropyl alcohol results in fast initiation of reaction and its completion in less than 2 min. Addition of acetone results in slower reaction with low reaction yield. Contrary to dry distilled THF, as-received solvent gives the effect similar to acetone (see Figure S3 in the Supporting Information). The difference between purified and as-received THF can be attributed to the presence of various impurities in as-received THF such as water, hydroperoxides, butyric acid, and related compounds.²³

Several mechanisms can be considered in order to explain the effect of alcohols on PbS nanocrystals growth. At first, it can be assumed that the nanoparticle production is triggered by the supersaturation formed by rapid drop in temperature of reaction mixture due to the injection of promoter. However, the absence of the effect in case of THF injection means that supersaturation does not play important role. The same negative result was observed for heptane (see Figure S4 in the Supporting Information): after heptane injection no reaction occurs even after 15 min at $60\text{ }^{\circ}\text{C}$. Moreover, PbS nanoparticles could be formed by adding isopropyl alcohol or acetone to the solution at as low temperatures as $30\text{ }^{\circ}\text{C}$, when the relative drop in temperature would be negligible (the temperatures lower than $30\text{ }^{\circ}\text{C}$ were not tested because of the precipitation of lead oleate from ODE solution¹⁶).

Another possible explanation involves the aggregative nanoparticle growth. After $(\text{TMS})_2\text{S}$ injection small “cluster-

like" PbS particles may be formed. They are relatively stable due to the passivation of their surface by oleic acid. Upon the addition of solvent these small particles begin to aggregate and recrystallize forming larger PbS nanoparticles. This mechanism explains the difference in the solvents behavior: isopropyl alcohol and acetone are more polar ($\epsilon = 18.3$ and 20.7 , respectively) than THF ($\epsilon = 7.4$) and widely used for QDs precipitation from nonpolar solvents. However, this assumption does not explain the different reactivity of dry distilled and as-received THF. Moreover, we observed nanoparticles formation even upon injection of as small alcohol amounts as $100\ \mu\text{L}$ which is inconsistent with the aggregative growth mechanism under consideration while such alcohol amounts are unlikely to cause aggregation of primary seeds. The difference between chemical action of polar protic alcohol and aprotic THF on the formation of PbS nanocrystals relates probably to the reaction of injected solvent and intermediate complex formed by lead oleate and $(\text{TMS})_2\text{S}$. Figure 3c demonstrates the appearance of induced optical absorption around $\lambda \approx 350\ \text{nm}$ after $(\text{TMS})_2\text{S}$ injection. This broad band cannot be attributed to $(\text{TMS})_2\text{S}$ itself²⁴ (absorption spectra of ODE and ODE- $(\text{TMS})_2\text{S}$ mixture are presented in Figure S5 of the Supporting Information). We suppose that this band could be assigned to the molecular complex **1** formed by the reaction shown in Scheme 1.

Scheme 1. Reaction of Lead Oleate with Bis(trimethylsilyl) Sulfide in an Inert Solvent

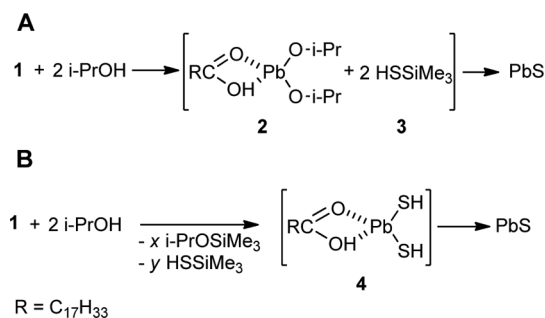


Similar complexes were reported to be formed by the reaction between silylated phosphines and indium compounds^{25,26} and Cd- and Zn-acetates with bis(trimethylsilyl) sulfide.^{24,27} Unfortunately, we failed to isolate and study the structure of lead oleate- $(\text{TMS})_2\text{S}$ complex due to its instability.

This reaction allows to understand the role of free oleic acid in the inhibition of reaction between $\text{Pb}(\text{oleate})_2$ and $(\text{TMS})_2\text{S}$. According to DeGroot and Corrigan,²⁴ the presence of donor ligand (in our case oleic acid) favors the formation of the monomeric complexes $\text{L}_2\text{M}(\text{SSiMe}_3)_2$ (where L stands for ligand and M for metal). Similar preparative procedures involving alcoholysis of silylated precursors were implemented for the preparation of nanoscale phosphides, and two possible reaction pathways were suggested.^{25,26} On the basis of these mechanisms, we propose possible reaction pathways for complex **1** with *i*-PrOH (see Scheme 2).

Theopold and Douglas²⁵ followed the reaction of dimeric $[\text{RR}'\text{InP}(\text{SiMe}_3)_2]_2$ ($\text{R} = \text{Cp}^*$, $\text{R}' = \text{Cl}$; $\text{R}, \text{R}' = \text{Me}_3\text{SiCH}_2$, $\text{R} = \text{Me}_3\text{SiCH}_2$, $\text{R}' = \text{Cl}$; $\text{R}, \text{R}' = \text{Me}_3\text{CCH}_2$) with methanol and *tert*-butanol with the aid of ^1H and ^{31}P NMR and came to the conclusion that the action of alcohol on **1** results in In–P (in our case Pb–S) bond cleavage yielding $\text{RR}'\text{InOMe}$ and $\text{HP}(\text{SiMe}_3)_2$, which subsequently convert into InP nanoparticles (see Scheme 2A). Matchett et al.²⁶ in their experiments with Cd_3P_2 nanoparticles implied that the mechanism described above could only be adopted when alkyl chains were used as metal ligands. For the alcoholysis of metal complexes with (trimethylsilyl)phosphines they suggested the mechanism resembling sol–gel processing of metal

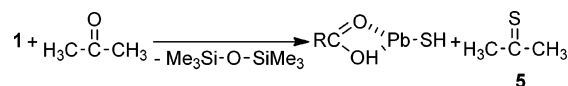
Scheme 2. Possible Reaction Mechanisms for PbS Nanocrystals Formation Promoted by Isopropyl Alcohol



oxides with the hydrolysis of alkoxide precursors (see Scheme 2B). At the first stage P–Si bond cleavage occurs with the formation of species similar to **4** which transform into metal phosphides in the polycondensation process.

The synthesis under consideration may not require the injection of only protic solvents, like alcohols and water. Although injection of acetone instead of *i*-PrOH ends up with practically the same result, but at slower rate, its reaction with **1** could not be described by Scheme 2. It is known that carbonyls with bis(trimethylsilyl) sulfide convert into thiocarbonyls.²⁸ Taking this into account, we may suggest slightly different reaction route (Scheme 3).

Scheme 3. Possible Reaction Mechanism for PbS Nanoparticles Formation with Acetone



Similar to process described in Scheme 2, the acetone addition on the first stage results in the cleavage of the Pb–S bond with the formation of highly reactive thioacetone **5** or similar compound which then reacts with Pb-containing species.

One may conclude that oleic acid itself as protic substance should promote the reaction similar to alcohols. However, bulky oleate and trimethylsilyl groups shield Pb–S “core” of **1**, thus preventing their reaction with the excess of oleic acid due to steric hindrances. In contrast to oleic acid, the molecule of the isopropyl alcohol is relatively small so, it can react with **1**, yielding reactive species that subsequently convert into PbS nanoparticles. In order to prove this idea, we also carried out experiments with $\text{Pb}(\text{2-ethylhexanoate})_2$ as Pb source (see Figure 5). After the $(\text{TMS})_2\text{S}$ injection the reaction mixture immediately became light yellow and then light brown. Injection of *i*-PrOH right after $(\text{TMS})_2\text{S}$ rapidly yields the precipitate consisting of large aggregates of PbS nanoparticles. The appearance of broad featureless optical absorption points to the formation of polydisperse ensemble of PbS QDs. This experiment demonstrates a crucial role of long-chain oleic acid, as less reactive species and stronger stabilizer of growing PbS nanoparticles.

In contrast to isopropyl alcohol and acetone, THF does not react with $(\text{TMS})_2\text{S}$ and thus is used as its cosolvent.²⁹ However, one can see that THF injection leads to the change in absorption spectrum of **1** (Figure 3c). The broad band observed after the $(\text{TMS})_2\text{S}$ injection gradually disappears, and the resulting spectrum of the obtained mixture resembles

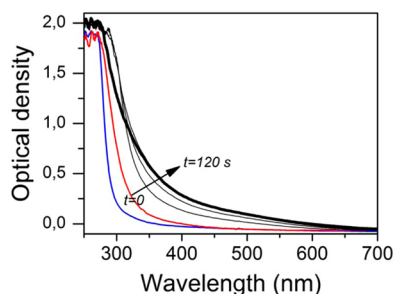


Figure 5. Optical absorption spectra of $\text{Pb}(\text{2-ethylhexanoate})_2$ solution in ODE before (blue line) and after $(\text{TMS})_2\text{S}$ injection (red line). Black lines represent the evolution of the absorbance spectra in time. Thin lines: spectra recorded every 5 s after injection. Bold line: resulting spectrum 2 min after the injection. The temperature of reaction $T = 50^\circ\text{C}$.

that for the lead oleate. Conversely, the injection of another “passive” compound—heptane—does not result in such changes in the absorption spectra. We attribute this effect to the ability of THF effectively solvate cations through interaction of oxygen atoms with metal atoms. In other words, although THF is incapable of cleaving S–Si bond in $(\text{TMS})_2\text{S}$ moiety, it breaks Pb–S bond forming unreactive complex, while $(\text{TMS})_2\text{S}$ is consumed in reactions with other components of the reactive mixture, i.e., oleic acid.

The different reactivity of thioacetone and HSSiMe_3 or H_2S (Schemes 2 and 3) also explains the difference in the final particle size (Figure 3a,b). While, more reactive thioacetone is consumed during the QD nucleation phase giving smaller nanocrystals, less reactive HSSiMe_3 governs further growth of PbS QDs.

The versatility of presented approach to the nanoparticles formation can be demonstrated when $\text{Pb}(\text{oleate})_2$ is substituted with $\text{Cd}(\text{oleate})_2$. Early reports on CdS nanoparticles preparation employing $(\text{TMS})_2\text{S}$ as S-source required $\text{Cd}(\text{CH}_3)_2$ as Cd-source and much higher temperatures (220°C).³⁰ Our method allows substantially decrease the reaction temperature and substitute pyrophoric dimethylcadmium with “greener” cadmium oleate. Figure 6 presents absorption spectra of $\text{Cd}(\text{oleate})_2$ solution before (blue curve) and after subsequent injection of $(\text{TMS})_2\text{S}$ first (red curve) and then isopropyl alcohol (black curve).

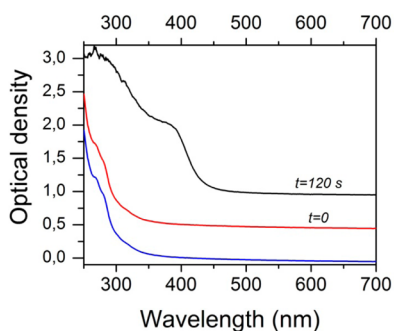


Figure 6. Optical absorption of reaction mixture containing $\text{Cd}(\text{oleate})_2$ solution in ODE before (blue line) and after (red line) $(\text{TMS})_2\text{S}$ injection. Black line: absorption spectrum of the reaction mixture 2 min after i-PrOH addition. The temperature of reaction $T = 50^\circ\text{C}$.

Similarly to PbS the formation of relatively stable complex analogous to **1** could be assumed. However, unlike lead oleate we did not detect the appearance of additional absorption related to the formation of complex between $\text{Cd}(\text{oleate})_2$ and $(\text{TMS})_2\text{S}$ perhaps due to the fact that cadmium complex absorbs at higher energies than lead-containing one. Again, the reaction of CdS QDs formation is not observed until isopropyl alcohol as promoter introduced. However, in the case of $\text{Cd}(\text{oleate})_2$ the injection of i-PrOH yields a considerable amount of CdS aggregates which may arise from different passivation of intermediates and growing CdS nanoparticles by oleic acid.

CONCLUSIONS

In summary, the reaction between lead oleate and bis-(trimethylsilyl) sulfide in octadecene at a temperature as low as 50°C can be strongly promoted by addition of protic solvents (alcohols, water) and acetone, resulting in the formation of ultrasmall PbS colloidal nanocrystals. The proposed mechanism involves formation of the $\text{Pb}(\text{oleate})_2$ - $(\text{TMS})_2\text{S}$ complex that upon the injection of the protic solvent forms highly reactive Pb- and S-containing intermediates. The different reactive ability of these intermediates allows to prepare PbS QDs of different size. Such a mild-temperature process is suitable for production of ultrasmall monodisperse PbS colloidal quantum dots because of suppressed recrystallization of PbS nanoparticles. Although this paper provides extensive data concerning the nanoparticles preparation, further study is required in order to transform our approach into reliable and reproducible synthetic protocol.

ASSOCIATED CONTENT

Supporting Information

Energy dispersive X-ray spectrum of PbS powder, TEM image, absorption spectra of $(\text{TMS})_2\text{S}$ solution in ODE, and reaction mixture after the injection of heptane and as-received THF. This material is available free of charge via the Internet at <http://pubs.acs.org>.

AUTHOR INFORMATION

Corresponding Author

*E-mail: m_artemyev@yahoo.com (M.A.).

Notes

The authors declare no competing financial interest.

ACKNOWLEDGMENTS

We thank A. Lyakhov for XRD and K. Skrotskaya for TEM measurements. This work was supported by the CHEMRE-AGENTS program.

REFERENCES

- (1) Semonin, O. E.; Luther, J. M.; Choi, S.; Chen, H.-Y.; Gao, J.; Nozik, A. J.; Beard, M. C. Peak External Photocurrent Quantum Efficiency Exceeding 100% via MEG in a Quantum Dot Solar Cell. *Science* **2011**, *334*, 1530–1533.
- (2) Sukhovatkin, V.; Hinds, S.; Brzozowski, L.; Sargent, E. H. Colloidal Quantum-Dot Photodetectors Exploiting Multiexciton Generation. *Science* **2009**, *324*, 1542–1544.
- (3) Wise, F. W. Lead Salt Quantum Dots: the Limit of Strong Quantum Confinement. *Acc. Chem. Res.* **2000**, *33*, 773–780.
- (4) Litvin, A. P.; Parfenov, P. S.; Ushakova, E. V.; Fedorov, A. V.; Artemyev, M. V.; Prudnikau, A. V.; Golubkov, V. V.; Baranov, A. V.

PbS Quantum Dots in a Porous Matrix: Optical Characterization. *J. Phys. Chem. C* **2013**, *117*, 12318–12324.

(5) Wang, Y.; Suna, A.; Mahler, W.; Kasowski, R. PbS in Polymers. From Molecules to Bulk Solids. *J. Chem. Phys.* **1987**, *87*, 7315–7322.

(6) Kane, R. S.; Cohen, R. E.; Silbey, R. Synthesis of PbS Nanoclusters within Block Copolymer Nanoreactors. *Chem. Mater.* **1996**, *8*, 1919–1924.

(7) Borrelli, N. F.; Smith, D. W. Quantum Confinement of PbS Microcrystals in Glass. *J. Non-Cryst. Solids* **1994**, *180*, 25–31.

(8) Berhanu, D.; Govender, K.; Smyth-Boyle, D.; Archbold, M.; Halliday, D. P.; O'Brien, P. A. Novel Soft Hydrothermal (SHY) Route to Crystalline PbS and CdS Nanoparticles Exhibiting Diverse Morphologies. *Chem. Commun.* **2006**, *45*, 4709–4711.

(9) Nenadovic, M. T.; Comor, M. I.; Vasic, V.; Mitic, O. I. Transient Bleaching of Small PbS Colloids. Influence of Surface Properties. *J. Phys. Chem.* **1990**, *94*, 6390–6396.

(10) Bakueva, L.; Gorelikov, I.; Musikhin, S.; Zhao, X. S.; Sargent, E. H.; Kumacheva, E. PbS Quantum Dots with Stable Efficient Luminescence in the Near-IR Spectral Range. *Adv. Mater.* **2004**, *16*, 926–929.

(11) Cademartiri, L.; Bertolotti, J.; Sapienza, R.; Wiersma, D. S.; Freymann, G.; Ozin, G. A. Multigram Scale, Solventless, and Diffusion-Controlled Route to Highly Monodisperse PbS. *J. Phys. Chem. B* **2006**, *110*, 671–673.

(12) Hines, M. A.; Scholes, G. D. Colloidal PbS Nanocrystals with Size-Tunable Near-Infrared Emission: Observation of Post-Synthesis Self-Narrowing of the Particle Size Distribution. *Adv. Mater.* **2003**, *15*, 1844–1849.

(13) Bolotin, I. L.; Asunskis, D. J.; Jawaid, A. M.; Liu, Y.; Snee, P. T.; Hanley, L. Effects of Surface Chemistry on Nonlinear Absorption, Scattering, and Refraction of PbSe and PbS Nanocrystals. *J. Phys. Chem. C* **2010**, *114*, 16257–16262.

(14) Joo, J.; Na, H. B.; Yu, T.; Yu, J. H.; Kim, Y. W.; Wu, F.; Zhang, J. Z.; Hyeon, T. Generalized and Facile Synthesis of Semiconducting Metal Sulfide Nanocrystals. *J. Am. Chem. Soc.* **2003**, *125*, 11100–11105.

(15) Moreels, I.; Justo, Y.; De Geyter, B.; Hastraete, K.; Martins, J. C.; Hens, Z. Size-Tunable, Bright, and Stable PbS Quantum Dots: A Surface Chemistry Study. *ACS Nano* **2011**, *5*, 2004–2012.

(16) Liu, T.-Y.; Li, M.; Ouyang, J.; Zaman, Md. B.; Wang, R.; Wu, X.; Yeh, C.-S.; Lin, Q.; Yang, B.; Yu, K. Non-Injection and Low-Temperature Approach to Colloidal Photoluminescent PbS Nanocrystals with Narrow Bandwidth. *J. Phys. Chem. C* **2009**, *113*, 2301–2308.

(17) Zhang, J.; Gao, J.; Miller, E. M.; Luther, J. M.; Beard, M. C. Diffusion-Controlled Synthesis of PbS and PbSe Quantum Dots with in Situ Halide Passivation for Quantum Dot Solar Cells. *ACS Nano* **2014**, *8*, 614–622.

(18) Abel, K. A.; Shan, J.; Boyer, J.-C.; Harris, F.; Veggel, F. C. J. M. Highly Photoluminescent PbS Nanocrystals: The Beneficial Effect of Trioctylphosphine. *Chem. Mater.* **2008**, *20*, 3794–3796.

(19) Ushakova, E. V.; Litvin, A. P.; Parfenov, P. S.; Fedorov, A. V.; Artemyev, M.; Prudnikau, A. V.; Rukhlenko, I. D.; Baranov, A. V. Anomalous Size-Dependent Decay of Low-Energy Luminescence from PbS Quantum Dots in Colloidal Solution. *ACS Nano* **2012**, *6*, 8913–8921.

(20) Warner, J. H.; Thomsen, E.; Watt, A. R.; Heckenberg, N. R.; Rubinshtein-Dunlop, H. Time-Resolved Photoluminescence Spectroscopy of Ligand-Capped PbS Nanocrystals. *Nanotechnology* **2005**, *16*, 175–179.

(21) Segets, D.; Lucas, J. M.; Taylor, R. N. K.; Scheele, M.; Zheng, H.; Alivisatos, A. P.; Peukert, W. Determination of the Quantum Dot Band Gap Dependence on Particle Size from Optical Absorbance and Transmission Electron Microscopy Measurements. *ACS Nano* **2012**, *6*, 9021–9032.

(22) Hens, Z.; Moreels, I. Light Absorption by Colloidal Semiconductor Quantum Dots. *J. Mater. Chem.* **2012**, *22*, 10406–10415.

(23) Coetzee, J. F.; Chang, T.-H. Purification of Solvents for Electroanalysis: Tetrahydrofuran and Dioxane. *Pure Appl. Chem.* **1985**, *57*, 633–638.

(24) DeGroot, M. W.; Corrigan, J. F. Coordination Complexes of Zinc with Reactive ESiMe_3 ($\text{E} = \text{S}, \text{Se}, \text{Te}$) Ligands. *Organometallics* **2005**, *24*, 3378–3385.

(25) Theopold, K. H.; Douglas, T. Molecular Precursors for Indium Phosphide and Synthesis of Small III-V Semiconductor Clusters in Solution. *Inorg. Chem.* **1991**, *30*, 594–596.

(26) Matchett, M. A.; Viano, A. M.; Adolphi, N. L.; Stoddard, R. D.; Buhro, W. E.; Conradi, M. S.; Gibbons, P. C. Sol-Gel-like Route to Crystalline Cadmium Phosphide Nanoclusters. *Chem. Mater.* **1992**, *4*, 508–511.

(27) DeGroot, M. W.; Taylor, N. J.; Corrigan, J. F. Controlled Synthesis of Ternary II–II'–VI Nanoclusters and the Effects of Metal Ion Distribution on Their Spectral Properties. *Inorg. Chem.* **2005**, *44*, 5447–5458.

(28) McGregor, W. M.; Sherrington, D. C. Some Recent Synthetic Routes to Thioketones and Thioaldehydes. *Chem. Soc. Rev.* **1993**, *22*, 199–204.

(29) Matulenko, M. A.; Degl'Innocenti, A.; Capperucci, A. *Bis(trimethylsilyl) Sulfide*. *e-EROS Encyclopedia of Reagents for Organic Synthesis*, 2007.

(30) Murray, C. B.; Norris, D. J.; Bawendi, M. G. Synthesis and Characterization of Nearly Monodisperse CdE ($\text{E} = \text{S}, \text{Se}, \text{Te}$) Semiconductor Nanocrystallites. *J. Am. Chem. Soc.* **1993**, *115*, 8706–8715.